Theory of deep impurity levels in CuCl

Shang-Yuan Ren,* Roland E. Allen,† and John D. Dow
Department of Physics and Materials Research Laboratory, University of Illinois at Urbana-Champaign, Urbana, Illinois 61801

I. Lefkowitz
U. S. Army Research Office, Research Triangle Park, North Carolina 22709 and Hunter College of the City University of New York, New York 10021 and University of North Carolina, Chapel Hill, North Carolina 27514

(Received 11 June 1981)

The theory of deep impurity levels is extended to semiconductors with d electrons. The major chemical trends are predicted for a large number of substitutional impurities in CuCl. Deep levels are found for S and Se impurities on the Cl site, but not for Ag or Au on the Cu site, in agreement with experiment. The theory also predicts no deep level for isolated O on the Cl site, thus supporting the conclusion that the observed O-related defect is not a simple substitutional impurity.

I. INTRODUCTION

CuCl has been reported to exhibit an anomalous diamagnetism that is reminiscent of superconductivity[1-3] and possibly associated with defects.[4] The importance of defect states is further emphasized by the occurrence of a broadened z_3 exciton line[5] in the same temperature region in which the diamagnetism is observed. This broadening has been variously related to defect states, free electron effects,[5] a defect-stabilized plasma state,[6] or a modified phonon spectrum.[4] In order to provide some theoretical guidance for experiments involving defects in CuCl,[4,7] we have extended the theory of substitutional impurities[8-10] to include d electrons on the cation site. We focus on the deep levels—i.e., the levels that are bound within the fundamental band gap predominantly by the central-cell defect potential.

The theory of impurities in sp^3-bonded covalent materials, as enunciated by Hjalmarson *et al.*,[8] contains two basic ingredients: (i) an empirical tight-binding model of the host electronic structure that incorporates experimental information, chemical trends, and the relevant features of theoretical energy bands, and (ii) a defect potential whose off-diagonal matrix elements in the tight-binding basis are determined by Harrison's d^{-2} scaling rule[11] and whose diagonal matrix elements V_l are determined by the differences in impurity and host atomic energies:

$$V_l=\beta_l(E_l^i-E_l^h)\ . \tag{1.1}$$

Here E_l^i and E_l^h are impurity and host orbital energies for states of angular momentum l, and are converted into "orbital energies within the solid" by the constant factor β_l.

In this paper, we generalize the theory of Hjalmarson *et al.* to include d-electron orbitals on the cation site. This immediately leads to two changes: (i) The host Hamiltonian H_0 involves five d orbitals on the cation site, as well as one s orbital and three p orbitals on each site, and (ii) the defect potential matrix for Cu substitutional impurities is also augmented by matrix elements involving d orbitals.

II. THE MODEL

Our 13-state tight-binding host Hamiltonian is shown in Appendix A. Its parameters, given in Table I, were determined by a fitting procedure described in Appendix B. The resulting band structure is displayed in Fig. 1, together with the results of a psuedopotential calculation by Kleinman and Mednick.[12] The bands of Kunz *et al.*[13] and of Zunger and Cohen[14] are similar to those of Kleinman and Mednick.

The primary requirement of a successful tight-binding model is that it adequately reproduces the projected densities of states—not just the energy bands. It is these densities of states, for anion s and p electrons and for cation s, p, and d electrons, that determine the defect levels in accordance with Eqs. (3.2) and (3.3). We imposed the following re-

TABLE I. Parameters of the tight-binding model in eV. With these parameters the charges on the Cu and Cl ions are, respectively, $+0.59|e|$ and $-0.59|e|$.

$E(s,c)$	$E(s,a)$	$E(p,c)$	$E(p,a)$	$E(d,c)$	$E'(d,c)$	$V(x_c,yz_c)$	
2.80	−15.15	9.00	−3.75	−1.25	−1.90	0	
$V(s,s)$	$V(x_a,s_c)$	$V(s_a,x_c)$	$V(x,x)$	$V(x,y)$	$V_{sd\sigma}$	$V_{pd\sigma}$	$V_{pd\pi}$
−2.877	4.841	2.866	0	0	−1.980	−5.085	1.220

quirements in fitting our tight-binding model: (i) The band gap is 3.25 eV.[15] (ii) The Cu $3d$ bands lie above the Cl $3p$ bands,[16] and the widths of these bands[17] are approximately the observed widths. (iii) The four main peaks observed in x-ray photoemission[16] have their observed positions. (iv) The top of the highest valence band is 75% Cu $3d$ and 25% Cl $3p$.[16] (v) The charge on the Cu ion is positive. (vi) The remaining important features in the pseudopotential bands of Refs. 12–14 are adequately reproduced.

The resulting tight-binding Hamiltonian yields densities of state for the upper valence bands that are in good agreement with the available photoemission data, as shown in Table II and Fig. 2. It also produces bands that are in reasonable agreement with the pseudopotential calculations (Fig. 1).

III. METHOD OF CALCULATION

The change in the tight-binding Hamiltonian resulting from the introduction of an impurity or vacancy is the defect potential $V \equiv H - H_0$. If we neglect lattice relaxation, the defect potential is diagonal[8] because Harrison's scaling rules[11] imply that the off-diagonal matrix elements of H and H_0 are equal.

Following the approach of Hjalmarson *et al.*, we take the on-site diagonal defect potential for isoelectronic defects to be given by Eq. (1.1).[18] The Hjalmarson *et al.* model was originally developed for studying isoelectronic defects in highly covalent materials; its application to charged centers in more ionic materials requires a modification of the expression for V to account for the different ionic

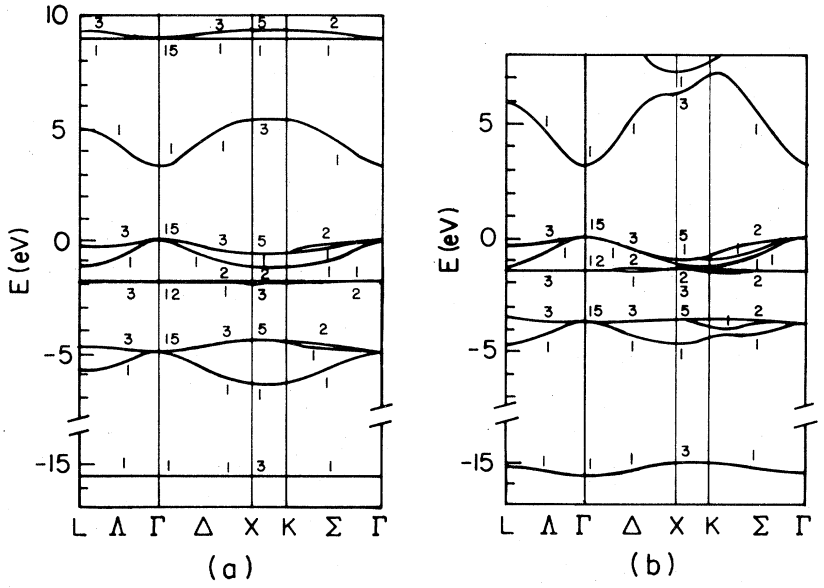

FIG. 1. Band structure of CuCl: (a) calculated from the Hamiltonian of Appendix A and Table I, (b) calculated by Kleinman and Mednick (Ref. 12).

TABLE II. Experimental features fit in determining the empirical CuCl Hamiltonian.

	Experiment	Theory
Order of valence bands	Cu $3d$ higher than Cl $3p$[a]	Cu $3d$ higher than Cl $3p$
Cu $3d$ character at top of valence band	75%[b]	75%
Cl $3p$ character at top of valence band	25%[b]	25%
Band gap (eV)	3.25[c]	3.25
Photoemission peaks (eV)		
A	0.8–1.4[b]	0.6
B	1.9–2.6[b]	1.9
C	4.9–5.2[b]	4.8
D	6.0–6.3[b]	6.4
Width of lower band (eV) (Cl $3p$)	2.4[a]	2.4
Width of upper band (eV) (Cu $3d$)	1.7[a]	2.0

[a]Reference 17.
[b]Reference 16.
[c]Reference 15.

charges. This modification we term ΔV_l; it is expected to have the same sign as the correction Eq. (1.1) would experience if ionic energies were used in place of atomic energies. Crude estimates of ΔV_l for singly charged defects in an ionic host such as CuCl indicate that it is of the order of 4 eV.[19] We shall see independently that a value of $\Delta V_p = 3.5$ eV produces S and Se levels in agreement with the data.

The defect potential for an anion-site defect is thus a diagonal 4×4 matrix with one element V_s and three elements V_p. For a cation-site defect, it is a 9×9 matrix with one element V_s, three elements V_p, three elements V_d, and two elements V_d'. (We do not assume that the d_{xy} and $d_{y^2-z^2}$ defect potentials are equal.) In each case we have

$$V_l = \beta_l(E_l^i - E_l^h) + \Delta V_l \ . \tag{3.1}$$

Since the defect potential is localized, it is appropriate to use the Green's-function method to compute the defect energy levels. This method produces a secular equation in a localized basis that involves only those basis functions within the defect space[8–10]:

$$\det[1 - G_0(E)V] = 0 \ , \tag{3.2a}$$

where we have

$$G_0(E) \equiv (E - H_0)^{-1} \ . \tag{3.2b}$$

For the anion site, this 4×4 problem reduces to four 1×1 problems, yielding one A_1 (s-like) and three degenerate T_2 (p-like) defect states. For the cation site, Eq. (3.2) is a 9×9 problem. Our decoupling of the cation p and d orbitals (see Appendix B) reduces Eq. (3.2) to nine scalar problems, yielding one A_1 (s-like), three T_2 (p-like), another three T_2 (d_{xy}-like), and two E ($d_{y^2-z^2}$-like) states.

Each eigenvalue problem has the form

$$\frac{1}{V_{\lambda b}} = G_{\lambda b}(E) = \int \frac{D_{\lambda b}(E')dE'}{E - E'} \ , \tag{3.3}$$

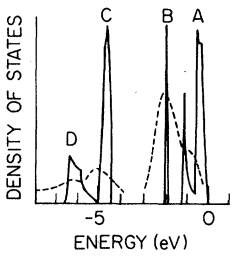

FIG. 2. Valence-band density of states calculated from the host Hamiltonian of this paper (solid curve), in comparison with the deconvoluted x-ray-photoelectron-spectroscopy spectra obtained by S. Kono *et al.* as cited in Ref. 16 (dashed curve).

where

$$\lambda = A_1(s),\ T_2(p),\ T_2(d_{xy}),\ \text{or}\ E(d_{y^2-z^2})\ , \tag{3.4}$$

and b means "anion" or "cation."

Here $D_{\lambda b}$ is the contribution of the λ-symmetric irreducible representation to the local density of states on the b site:

$$D_{\lambda b}(E) = \langle \lambda b \mid \delta(E - H_0) \mid \lambda b \rangle = \sum_{n\vec{k}} \langle \lambda b \mid n\vec{k} \rangle \langle n\vec{k} \mid \lambda b \rangle \delta(E - E_{n\vec{k}})\ . \tag{3.5}$$

IV. RESULTS

The predictions for deep levels associated with isolated substitutional impurities are given in Figs. 3–8. The predicted level for a given impurity is obtained from the intersection of the calculated curve with a vertical line representing the isoelectronic impurity potential.

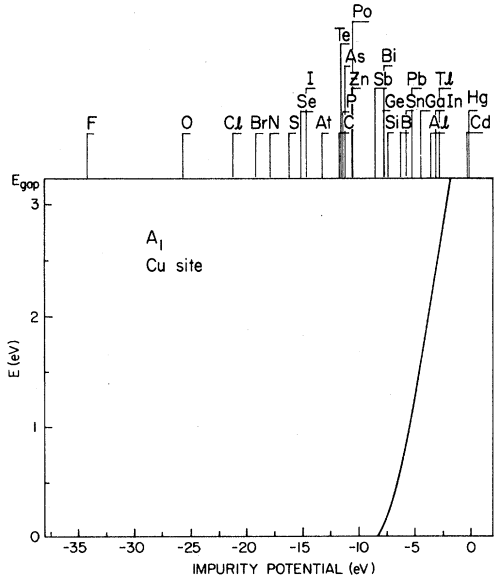

FIG. 3. Energies in eV of the A_1 (s-like) substitutional defect levels predicted for impurities at the Cu site in CuCl. The abscissa is the defect potential; each impurity has a tic at its potential. All transition-metal potentials are between -2 and $+2$ eV; hence these defects are not predicted to produce A_1 deep traps. No A_1 deep levels are predicted to lie within the band gap for the isoelectronic impurities Ag and Au.

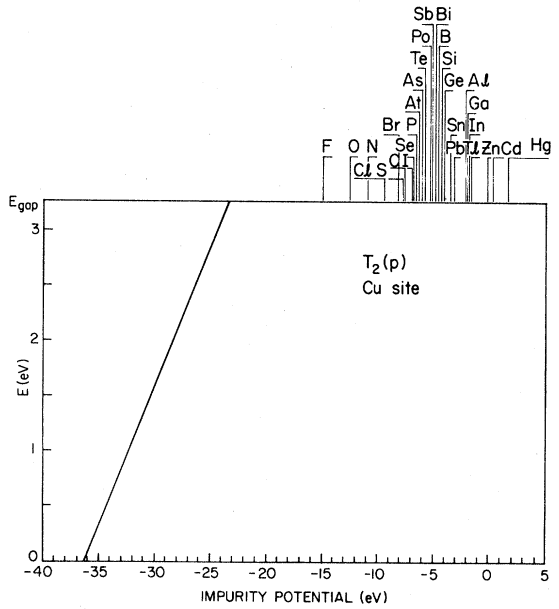

FIG. 4. Energies of the T_2 (p-like) substitutional defect levels predicted for impurities at the Cu site in CuCl. T_2 p-derived levels in the gap are not predicted for any of the impurities.

These predictions should be viewed within the context of the goals of the theory. They represent a global view of the expected chemical trends in the defect data, and should be corrected for the different charge states of the defect levels, and, possibly, lattice relaxation. (The present calcula-

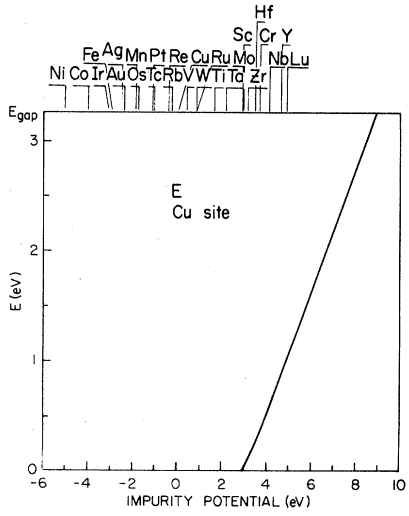

FIG. 5. Energies of the E-symmetric ($d_{y^2-z^2}$-like) defect levels predicted for impurities at the Cu site in CuCl. Notice that Ag and Au do not produce d-like E defect levels in the gap when on the Cu site.

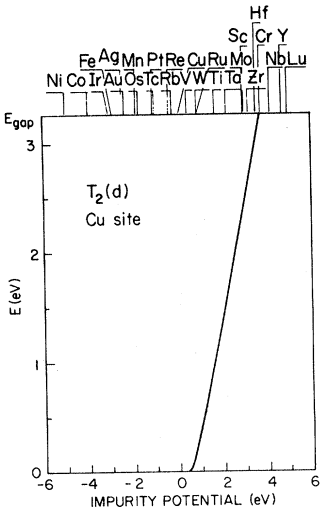

FIG. 6. T_2-symmetric (d_{xy}-like) defect levels for the Cu site. Note that Ag and Au again do not produce levels in the gap.

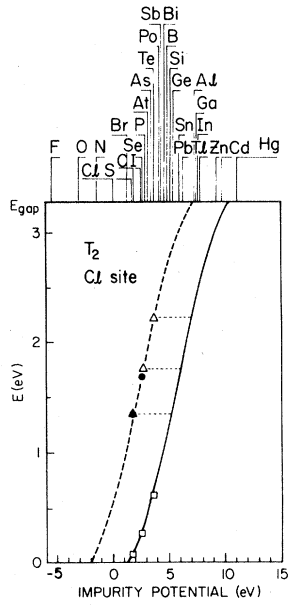

FIG. 8. Energies of the T_2 defect levels predicted for impurities on the Cl site of CuCl. The solid line is the uncorrected theory; the points marked with open squares are the uncorrected predictions for S, Se and Te levels. The solid circles represent the experimental results for S and Se (after Ref. 20). The dashed line represents the corrected theory for acceptors, with the correction being determined by the S datum; the open triangles are the corrected predictions for S, Se, and Te.

tions predict the neutral defect levels, and corrections to these levels for the different charge states can be estimated using simple electrostatic arguments.) Since the purpose of the theory is to predict trends, predictions of relative orderings of energy levels produced by different defects should be even more reliable than the theoretical energies of individual defects.

The predictions of the theory agree with the major experimental facts of which we are aware: (i) S and Se substituting for Cl are known to produce deep levels in CuCl,[20,21] with the Se level being 0.32 eV above the S level; (ii) searches for deep traps associated with Ag or Au substituting for Cu have been unsuccessful[22]; and (iii) an O-related level has been identified[20] which, unlike the S and Se levels, is not associated with the tetrahedral symmetry of a simple substitutional defect.

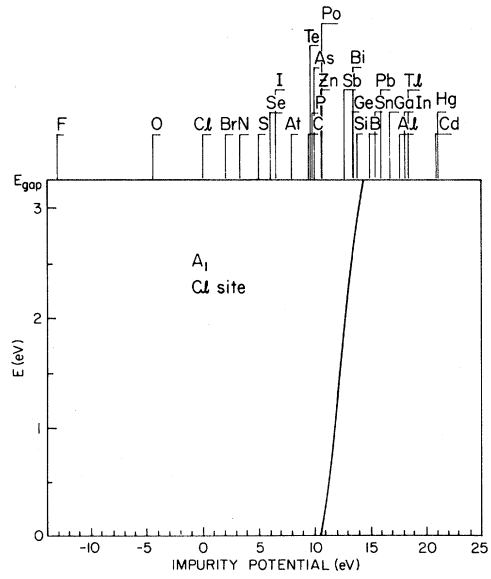

FIG. 7. Energies of the A_1 defect levels predicted for impurities on the Cl site of CuCl.

The experimental S and Se impurity levels have the same ordering as in the uncorrected predictions of Fig. 8, but are somewhat higher in absolute energy than predicted. As mentioned in Sec. III, the uncorrected predictions are for isoelectronic impurities [Eq. (1.1)], whereas the S and Se impurities are expected to have an extra electron in comparison with the replaced Cl atom. (Roughly speaking, S^- and Se^- replace Cl^-.) Allowance for the fact that S is not isoelectronic to Cl, through modification of the defect potential as prescribed in (3.1), brings the theory into improved agreement with the data. By choosing the defect potential modification ΔV_p such that the S datum is reproduced, we find a reasonable value $\Delta V_p = 3.5$ eV. The correction ΔV_p contains not only the atomistic

correction discussed above, but the long-range polarization energy, which systematically alters the levels of the S, Se, and Te defects. We then predict a Se level in excellent agreement with the observed value, as indicated in Fig. 8. Such agreement is, of course, expected of a theory that is intended to predict trends in impurity levels more reliably than absolute energies.[8]

The theory predicts that the defect levels associated with Ag or Au on the Cu site all lie within the bands and outside of the fundamental band gap. Thus it explains why no deep levels have been observed for these impurities.[22]

An especially interesting prediction of the model is that isolated O on a Cl site should not produce a deep trap, but its isoelectronic mates S and Se should. The reason for this is that O attracts electrons more strongly than Cl, whereas S and Se are weaker. The O levels should therefore lie below the corresponding Cl levels, outside the gap, whereas the S and Se levels should lie above Cl, within the gap. Thus, in a natural way, the theory supports the interpretation that the O-related defect, with a level 1.08 eV above the valence band,[20] is not a substitutional impurity like S and Se, but is instead an extended defect of nontetrahedral symmetry. The present work, therefore, lends indirect support to the work of Kunz *et al.*,[13] who have proposed that a complex consisting of O^{-2} and a vacancy produces a level near the conduction-band edge.

Finally, when it substitutes for Cl, the impurity Te should produce a T_2-symmetric defect level at about 2.20 eV above the valence-band edge. Observation of this level would provide gratifying confirmation of the present theory.

ACKNOWLEDGMENTS

We thank O. F. Sankey for his many enlightening comments, and we acknowledge the Office of Naval Research (Grant No. ONR-N-00014-77-C-0537) for support, and the Materials Research Laboratory for the use of their computer (Department of Energy Grant No. DE-AC02-76-ER01198).

APPENDIX A

The 13-orbital tight-binding Hamiltonian has the form as shown in Table III, where we have

$$g_0=\cos q_1\cos q_2\cos q_3-i\sin q_1\sin q_2\sin q_3\ , \tag{A1a}$$

$$g_1=-\cos q_1\sin q_2\sin q_3+i\sin q_1\cos q_2\cos q_3\ , \tag{A1b}$$

$$g_2=-\sin q_1\cos q_2\sin q_3+i\cos q_1\sin q_2\cos q_3\ , \tag{A1c}$$

$$g_3=-\sin q_1\sin q_2\cos q_3+i\cos q_1\cos q_2\sin q_3 \tag{A1d}$$

with

$$\vec{q}=\frac{a}{4}\vec{k}$$

and

$$V(s_a,xy_c)=\frac{1}{\sqrt{3}}V_{sd\sigma}\ , \tag{A2a}$$

$$V(x_a,xy_c)=\tfrac{1}{3}V_{pd\sigma}+\frac{1}{3}\frac{1}{\sqrt{3}}V_{pd\pi}\ ,$$

$$V(x_a,yz_c)=\tfrac{1}{3}V_{pd\sigma}-\frac{2}{3}\frac{1}{\sqrt{3}}V_{pd\pi}\ , \tag{A2b}$$

TABLE III. 13-orbital tight-binding Hamiltonian matrix.

	s_a	s_c	x_a	y_a	z_a	x_c	y_c
s_a	$E(s,a)$	$V(s,s)g_0^*$	0	0	0	$-V(s_a,x_c)g_1^*$	$-V(s_a,x_c)g_2^*$
s_c	$V(s,s)g_0$	$E(s,c)$	$V(s_c,x_a)g_1$	$V(s_c,x_a)g_2$	$V(s_c,x_a)g_3$	0	0
x_a	0	$V(s_c,x_a)g_1^*$	$E(p,a)$	0	0	$V(x,x)g_0^*$	$V(x,y)g_3^*$
y_a	0	$V(s_c,x_a)g_2^*$	0	$E(p,a)$	0	$V(x,y)g_3^*$	$V(x,x)g_0^*$
z_a	0	$V(s_c,x_a)g_3^*$	0	0	$E(p,a)$	$V(x,y)g_2^*$	$V(x,y)g_1^*$
x_c	$-V(s_a,x_c)g_1$	0	$V(x,x)g_0$	$V(x,y)g_3$	$V(x,y)g_2$	$E(p,c)$	0
y_c	$-V(s_a,x_c)g_2$	0	$V(x,y)g_3$	$V(x,x)g_0$	$V(x,y)g_1$	0	$E(p,c)$
z_c	$-V(s_a,x_c)g_3$	0	$V(x,y)g_2$	$V(x,y)g_1$	$V(x,x)g_0$	0	0
x_cy_c	$V(s_a,xy_c)g_3$	0	$-V(x_a,xy_c)g_2$	$-V(x_a,xy_c)g_1$	$-V(x_a,yz_c)g_0$	0	0
y_cz_c	$V(s_a,xy_c)g_1$	0	$-V(x_a,yz_c)g_0$	$-V(x_a,xy_c)g_3$	$-V(x_a,xy_c)g_2$	$V(x_c,yz_c)$	0
x_cz_c	$V(s_a,xy_c)g_2$	0	$-V(s_a,xy_c)g_3$	$-V(x_a,yz_c)g_0$	$-V(x_a,xy_c)g_1$	0	$V(x_c,yz_c)$
$y_c^2-z_c^2$	0	0	0	$-V(y_a,y^2-z_c^2)g_2$	$V(y_a,y^2-z_c^2)g_3$	0	0
$3x_c^2-r_c^2$	0	0	$2V(y_a,3x^2-r_c^2)g_1$	$-V(y_a,3x^2-r_c^2)g_2$	$-V(y_a,3x^2-r_c^2)g_3$	0	0

$$V(y_a,y^2-z_c^2)=\frac{1}{\sqrt{3}}V_{pd\pi}\,,$$

$$V(y_a,3x^2-r_c^2)=-\tfrac{1}{3}V_{pd\pi}\,. \qquad \text{(A2c)}$$

APPENDIX B

As discussed in the text, our first priority in fitting the tight-binding Hamiltonian is to reproduce the available experimental data. A second priority is to fit the remaining important features of the bands obtained in the pseudopotential calculations of Refs. 12 and 14.

We first take

$$V(x_c,yz_c)=0\,. \qquad \text{(B1)}$$

There are three reasons for doing this: (i) Preliminary fits indicated that this parameter should have a small value, of the order of 0.1 eV. This is to be expected because the coupling vanishes in the free Cu atom. (ii) Equation (B1) reduces the band fitting to an entirely linear procedure, with none of the ambiguities that can plague nonlinear fits. (iii) The impurity problem is reduced to the solution of scalar equations. With $V(x_c,yz_c)\neq 0$, the impurity problem on the cation site involves three 1×1 secular equations (corresponding to s, $d_{y^2-z^2}$, and $d_{3x^2-r^2}$ electrons) and three 2×2 equations (corresponding to p_x and d_{yz}, p_y and d_{xz}, and p_z and d_{xy} electrons). But with $V(x_c,yz_c)=0$, the p and d electrons are decoupled, and this problem reduced to nine 1×1 problems.

The matrix elements $E(s,c)$, $E(s,a)$, $E(p,c)$, $E(p,a)$, $E(d,c)$, $E'(d,c)$, $V(s,s)$, $V(x,x)$, $V(x_c,yz_c)$, and $V(x_a,yz_c)$ are determined by fitting information about the band structure at Γ, the center of the Brillouin zone. According to group theory, there are three Γ_{15} states. Their energies are determined by the equation:

$$\begin{vmatrix} E(p,a)-E & V(x,x) & -V(x_a,yz_c) \\ V(x,x) & E(p,c)-E & 0 \\ -V(x_a,yz_c) & 0 & E(d,c)-E \end{vmatrix}=0\,. \qquad \text{(B2)}$$

Experimentally[16] the wave function at the top of the valence band (Γ_{15}) is composed of 25% Cl $3p$, 75% Cu $3d$, and a negligible percentage of Cu $4p$. To eliminate the Cu $4p$ contribution at the valence-band maximum, we first choose $V(x,x)=0$. The remaining off-diagonal parameter $V(x_a,yz_c)$ is then fixed by requiring that the 25% Cl $3p$ and 75% Cu $3d$ character be reproduced. The diagonal matrix elements $E(p,a)$ and $E(d,c)$ are chosen so that the energy at the top of the valence band is zero and the lower Cl $3p$-like valence band (also Γ_{15}) occurs at -5 eV, in agreement with photoemission data. This leaves $E(p,c)$ to be determined.

The matrix element $E'(d,c)$ can be determined by the position of peak B of the photoemission data (Fig. 2), which corresponds to the Γ_{12} valence band. The matrix elements $E(s,c)$, $E(s,a)$, and $V(s,s)$ determine the bottoms of the conduction band and the lowest valence band, both of which are Γ_1. The bottom of the conduction band is given by the experimental band gap (3.25 eV), and the bottom of the lowest valence band is taken from the calculation of Kleinman and Mednick. The third of these parameters is fixed by requiring the lowest valence band to have 90% Cl $3s$ charac-

TABLE II. *(Continued.)*

z_c	x_cy_c	y_cz_c	x_cz_c	$y_c^2-z_c^2$	$3x_c^2-r_c^2$
$-V(s_a,x_c)g_3^*$	$V(s_a,xy_c)g_3^*$	$V(s_a,xy_c)g_1^*$	$V(s_a,xy_c)g_2^*$	0	0
0	0	0	0	0	0
$V(x,y)g_2^*$	$-V(x_a,yz_c)g_2^*$	$-V(x_a,yz_c)g_0^*$	$-V(x_a,xy_c)g_3^*$	0	$2V(y_a,3x^2-r_c^2)g_1^*$
$V(x,y)g_1^*$	$-V(x_a,xy_c)g_1^*$	$-V(x_a,xy_c)g_3^*$	$-V(x_a,yz_c)g_0^*$	$-V(y_a,y^2-z_c^2)g_2^*$	$-V(y_a,3x^2-r_c^2)g_2^*$
$V(x,x)g_0^*$	$-V(x_a,yz_c)g_0^*$	$-V(x_a,xy_c)g_2^*$	$-V(x_a,xy_c)g_1^*$	$V(y_a,y^2-z_c^2)g_3^*$	$-V(y_a,3x^2-r_c^2)g_3^*$
0	0	$V(x_c,yz_c)$	0	0	0
0	0	0	$V(x_c,yz_c)$	0	0
$E(p,c)$	$V(x_c,yz_c)$	0	0	0	0
$V(x_c,yz_c)$	$E(d,c)$	0	0	0	0
0	0	$E(d,c)$	0	0	0
0	0	0	$E(d,c)$	0	0
0	0	0	0	$E'(d,c)$	0
0	0	0	0	0	$E'(d,c)$

ter, as calculated by Zunger and Cohen.[14]

The matrix element $E(p,c)$ is fitted to the previously calculated results for the highest conduction bands (Γ_{15}) at Γ.[12,14] The remaining matrix elements are determined by fitting previously calculated results at the X point. In our model, the secular equations at the X point are

$$\begin{vmatrix} E(s,c)-E & iV(x_a,s_c) & 0 \\ iV(x_a,s_c) & E(p,a)-E & i\frac{2}{3}V_{pd\pi} \\ 0 & -i\frac{2}{3}V_{pd\pi} & E'(d,c)-E \end{vmatrix}=0 , \quad \text{(B4)}$$

for X_1,

$$E'(d,c)-E=0 , \quad \text{(B5)}$$

for X_2,

$$\begin{vmatrix} E(s,a)-E & iV(x_c,s_a) & iV_{sd\sigma}/\sqrt{3} \\ -iV(x_c,s_a) & E(p,c)-E & 0 \\ -iV_{sd\sigma}/\sqrt{3} & 0 & E(d,c)-E \end{vmatrix}=0 , \quad \text{(B6)}$$

for X_3, and

$$\begin{vmatrix} E(p,c)-E & iV(x,y) & 0 \\ -iV(x,y) & E(p,a)-E & i\left[\frac{1}{3}V_{pd\sigma}+\frac{1}{3}\frac{1}{\sqrt{3}}V_{pd\pi}\right] \\ 0 & -i\left[\frac{1}{3}V_{pd\sigma}+\frac{1}{3}\frac{1}{\sqrt{3}}V_{pd\pi}\right] & E(d,c)-E \end{vmatrix}=0 \quad \text{(B7)}$$

for X_5. From these equations, the off-diagonal matrix elements can be determined directly:

$$[V(x_a,s_c)]^2=-\frac{[E(s,c)-X_1(1)][E(s,c)-X_1(2)][E(s,c)-X_1(3)]}{E(s,c)-E'(d,c)} , \quad \text{(B8)}$$

$$(\tfrac{2}{3}V_{pd\pi})^2=-\frac{[E'(d,c)-X_1(1)][E'(d,c)-X_1(2)][E'(d,c)-X_1(3)]}{E(s,c)-E'(d,c)} , \quad \text{(B9)}$$

$$[V(x_c,s_a)]^2=-\frac{[E(p,c)-X_3(1)][E(p,c)-X_3(2)][E(p,c)-X_3(3)]}{E(p,c)-E(d,c)} , \quad \text{(B10)}$$

$$(V_{sd\sigma}^2/3)=-\frac{[E(d,c)-X_3(1)][E(d,c)-X_3(2)][E(d,c)-X_3(3)]}{E(p,c)-E(d,c)} , \quad \text{(B11)}$$

$$[V(x,y)]^2=-\frac{[E(p,c)-X_5(1)][E(p,c)-X_5(2)][E(p,c)-X_5(3)]}{E(p,c)-E(d,c)} , \quad \text{(B12)}$$

and

$$\left[\frac{1}{3}V_{pd\sigma}+\frac{1}{3}\frac{1}{\sqrt{3}}V_{pd\pi}\right]^2=-\frac{[E(d,c)-X_5(1)][E(d,c)-X_5(2)][E(d,c)-X_5(3)]}{E(p,c)-E(d,c)} . \quad \text{(B13)}$$

Here $X_i(j)$, with $i=1$, 3, and 5 and $j=1$, 2, and 3, are the three energy values of the X_i representation. We choose the $X_i(j)$ employing the following two conditions: (i) they should give a band structure which is in good agreement with previous calculations, and (ii) the tight-binding Hamiltonian should give a positive charge on the Cu site. Table I presents the parameters determined by this scheme.

*Permanent address: Department of Physics, University of Science and Technology of China, Hefei, China. Please send reprint requests to the Physics Department Reprint Secretary, Urbana.

†Permanent address: Department of Physics, Texas A&M University, College Station, Texas 77843.

[1]N. B. Brandt, S. V. Kuvshinnikov, A. P. Rusakov, and M. Semyonov, Zh. Eksp. Teor. Fiz. Pis'ma Red. 27, 37 (1978).

[2]C. W. Chu, A. P. Rusakov, S. Huang, S. Early, T. H. Geballe, and C. Y. Huang, Phys. Rev. B 18, 2116 (1978).

[3]I. Lefkowitz, J. S. Manning, and P. E. Bloomfield, Phys. Rev. B 20, 4506 (1979).

[4]I. Lefkowitz (unpublished).

[5]C. I. Yu, T. Goto, and M. Veta, J. Phys. Soc. Jpn. 34, 693 (1973).

[6]M. Combescot and C. Benoit a la Guillaume, Phys. Rev. Lett. 44, 182 (1980).

[7]D. C. Reynolds, R. J. Almasey, C. W. Litton, G. L. Koos, A. B. Kunz, and T. C. Collins, Phys. Rev. Lett 44, 204 (1980).

[8]H. P. Hjalmarson, P. Vogl, D. J. Wolford, and J. D. Dow, Phys. Rev. Lett. 44, 810 (1980).

[9]O. F. Sankey, H. P. Hjalmarson, J. D. Dow, D. J. Wolford, and B. G. Streetman, Phys. Rev. Lett. 45, 1656 (1980).

[10]R. E. Allen and J. D. Dow, J. Vac. Sci. Technol. 19, 383 (1981).

[11]W. A. Harrison, *Electronic Structure and the Properties of Solids* (Freeman, San Francisco, 1980).

[12]L. Kleinman and K. Mednick, Phys. Rev. B 20, 2487 (1979).

[13]A. B. Kunz, R. S. Weidman, and T. C. Collins, Int. J. Quantum Chem. Symp. 13, 453 (1979).

[14]A. Zunger and M. L. Cohen, Phys. Rev. B 20, 1189 (1979).

[15]H. Müller, S. Ves, H. D. Hoehheimer, M. Cardona, and A. Jayaraman, Phys. Rev. B 22, 1052 (1980).

[16]A. Goldmann, Phys. Status Solidi B 81, 9 (1977).

[17]G. van der Laan, G. A. Sawatzky, C. Haas, and H. W. Myron, Phys. Rev. B 20, 4287 (1979).

[18]For the highly covalent group-IV and III–V materials of Ref. 8, the choice of constants was $\beta_s=0.8$ and $\beta_p=0.6$. [See P. Vogl, H. P. Hjalmarson, and J. D. Dow (unpublished)]. For the more ionic I–VII materials of interest in the present paper, we choose $\beta_s=0.95$, $\beta_p=0.90$, and $\beta_d=1.00$.

[19]S.-Y. Ren (unpublished).

[20]A. Goltzene, O. Scherab, B. Meyer, and S. Nikitine, Opt. Commun. 5, 248 (1972).

[21]A. Goltzene, B. Meyer, C. Schwab, and K. Cho, Phys. Status Solidi B 69, 237 (1975).

[22]A. Goltzene and C. Schwab, Phys. Status Solidi B 71, K67 (1975).